# Materials Horizons



### COMMUNICATION

View Article Online



Cite this: DOI: 10.1039/d1mh01267c

Received 10th August 2021, Accepted 10th November 2021

DOI: 10.1039/d1mh01267c

rsc.li/materials-horizons

# Directly decorated CeY zeolite for $O_2$ -selective adsorption in $O_2/N_2$ separation at ambient temperature†

Hanbang Liu,<sup>ab</sup> Danhua Yuan,<sup>a</sup> Liping Yang,<sup>ab</sup> Jiacheng Xing,<sup>ab</sup> Shu Zeng,<sup>ab</sup> Shutao Xu, <sup>ba</sup> Yunpeng Xu <sup>ab</sup> and Zhongmin Liu <sup>bab</sup>

The traditional zeolites used in air separation are generally  $N_2$ -selective adsorbents. It was found for the first time that the  $O_2/N_2$  adsorption selectivity can be reversed by directly decorating the Ce metal ion sites of a traditional Y zeolite with imidazole molecules, which results in a novel  $O_2$  adsorbent. The  $O_2/N_2$  selectivity changes from 0.9 to 1.6 under normal conditions, and most importantly, the  $O_2$  adsorbent is recyclable. The *in situ* XPS characterization results indicate that the imidazole modification can change the electronic state of Ce in the Y zeolite and increase its affinity for  $O_2$ , which is confirmed by theoretical calculations. Dynamic breakthrough adsorption experiments show that the adsorbent has significant application potential in air separation.

 $O_2$  and  $N_2$  are widely used in numerous industrial and medical processes, and their separation from air is a very important and challenging endeavor. Currently, cryogenic distillation of air is the primary strategy for producing pure  $O_2$  and pure  $N_2$ , but this process is energy-consuming and costly. Therefore, low-energy consumption and low-cost separation processes based on porous adsorbents, such as pressure swing adsorption (PSA), which occurs near ambient temperature and pressure, have become attractive. Two kinds of adsorbents are commonly used in the air separation process:  $N_2$ -selective adsorbents and  $O_2$ -selective adsorbents. The proportion of  $O_2$  in the air is less than that of  $N_2$  (21% *versus* 78%); thus, the  $O_2$ -selective adsorbent and the length of the adsorption column in air separation, thereby reducing the equipment investment and energy

#### New concepts

As adsorbents that are low cost and have mature industrialized synthesis technologies, traditional zeolites usually have a high adsorption selectivity for some adsorbate molecules with high polarity or quadrupole moments because of their charge compensating metal cation sites. However, it will be more efficient if the zeolite preferentially adsorbs some other adsorbates in some actual separation processes, such as air separation based on O2-selective adsorption. In this work, a new concept was demonstrated in which directly decorating the metal cation sites of zeolites with organic ligands changes their properties to exhibit a unique adsorption ability towards some adsorbates that have low adsorption selectivity on traditional zeolites. Based on this method, the CeY zeolite decorated with imidazole has a special interaction with O2 and becomes an O2-selective adsorbent. The obtained adsorbent has an outstanding O2-selective adsorption capacity, dynamic O2/N2 separation performance and the ability to regenerate at ambient temperature, which has not been reported up to now in the field of zeolite research. Based on this strategy, it is believed that more types of metal sites within zeolites could be activated, and could be used in more adsorption and catalysis processes that require the participation of metal sites.

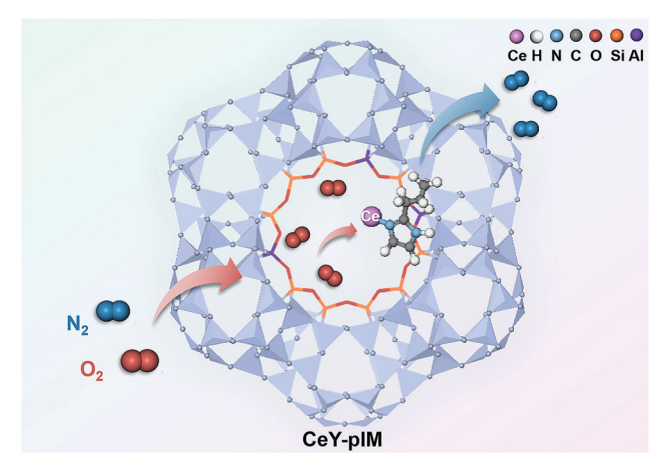
consumption, especially in pure N<sub>2</sub> production. 1,5-7 Among the O<sub>2</sub>-selective adsorbents, carbon molecular sieves (CMS) are the most widely used commercial O2-selective adsorbents that use kinetic strategies to adsorb O2, although precise control of the CMS pore size needs both an operator with rich experience and superb technology. 8,9 As potential O2 adsorbents, O2-binding cobalt complexes have been deeply studied in the last century. 10,11 However, the long-term chemical instability of the adsorbent is not satisfactory for its further utilization. In recent years, metal-organic frameworks (MOFs) with coordinatively unsaturated metal sites and tunable pore sizes have received widespread attention due to their O<sub>2</sub>-selective binding ability, which usually have high O<sub>2</sub> uptake and selectivity over N2 through chemical adsorption, but this adsorption is usually irreversible at room temperature, and most of these adsorbents are unstable in humid air. 12-15 Zeolite is a well-studied adsorbent in the field of air separation, and

<sup>&</sup>lt;sup>a</sup> National Engineering Laboratory for Methanol to Olefins, Dalian National Laboratory for Clean Energy, Dalian Institute of Chemical Physics, Chinese Academy of Sciences, Dalian 116023, P. R. China. E-mail: xuyunpeng@dicp.ac.cn

<sup>&</sup>lt;sup>b</sup> University of Chinese Academy of Sciences, Beijing 100049, P. R. China

 $<sup>\</sup>dagger$  Electronic supplementary information (ESI) available: Experimental, characterization and molecular simulation details, PXRD analysis, SEM images, TGA data,  $N_2$  and  $O_2$  adsorption isotherms at different temperatures, breakthrough cycle experiments, in situ Ce 3d XPS analysis, ICP-OES analysis and TOC results, and fitting parameters of the IAST model. See DOI: 10.1039/d1mh01267c

Communication Materials Horizons



Scheme 1 Schematic illustration of the  $O_2$ -selective adsorption process on imidazole-decorated CeY.

most zeolites are  $N_2$  selective because of the high quadrupole moment of  $N_2$  and the strong electric field of the zeolite framework. Only a few zeolites have achieved non-kinetic  $O_2$  selective adsorption, and their separation performance is not yet high enough for application.  $^{7,19}$ 

In past work, our group reported the strategy of introducing ZIF fragments into traditional zeolites.  $^{20,21}$  ZIF fragments have been proven to be effective tools for improving the selectivity of  $\mathrm{CH_4/N_2}$  as well as propylene/propane because the interaction between imidazole and  $\mathrm{CH_4}$  is stronger than the interaction with  $\mathrm{N_2}$  and because they achieve kinetic propylene/propane separation by modulating the pore size of the zeolite. In fact,

the properties of metal cation sites within zeolites also change after decoration with imidazole, thus affecting their interaction with adsorbate molecules. This work reports a new application of imidazole ligands in decorating traditional zeolites for air separation. The N2 adsorption capacity of FAU-type zeolites, such as zeolites X and Y, is significantly higher than that of O2, 22 and Ce ion-exchanged Y zeolites also have the same N2selective adsorption behavior. However, it was found in this study that the N<sub>2</sub>/O<sub>2</sub> selectivity is obviously reversed when CeY is modified with imidazole molecules (Scheme 1). The properties of CeY modification with several different imidazole molecules (mIM = 2-methylimidazole, eIM = 2-ethylimidazole and pIM = 2-propylimidazole) were investigated in the experiments. Static physical adsorption and dynamic breakthrough experiments were used to investigate the N2 and O2 adsorption capacity, selectivity and regeneration performance of CeY before and after modification. The physicochemical properties of the modified zeolites were characterized using FTIR, NMR and XPS and were correlated with their N2 and O2 adsorption performances. Finally, the mechanism for the O2 selectivity enhancement of the CeY zeolite modified with imidazole was analyzed using theoretical calculations.

The PXRD patterns (Fig. S2, ESI†) of all samples have typical characteristic peaks of the FAU structure, which suggests that ion exchange and the modification did not destroy the framework structure of the Y zeolite. The SEM images (Fig. S3, ESI†) showed that the morphology of the zeolite was maintained after modification. The Ce and C content of all the samples were tested using ICP-OES and TOC, respectively, and it was found that the C content of the decorated samples

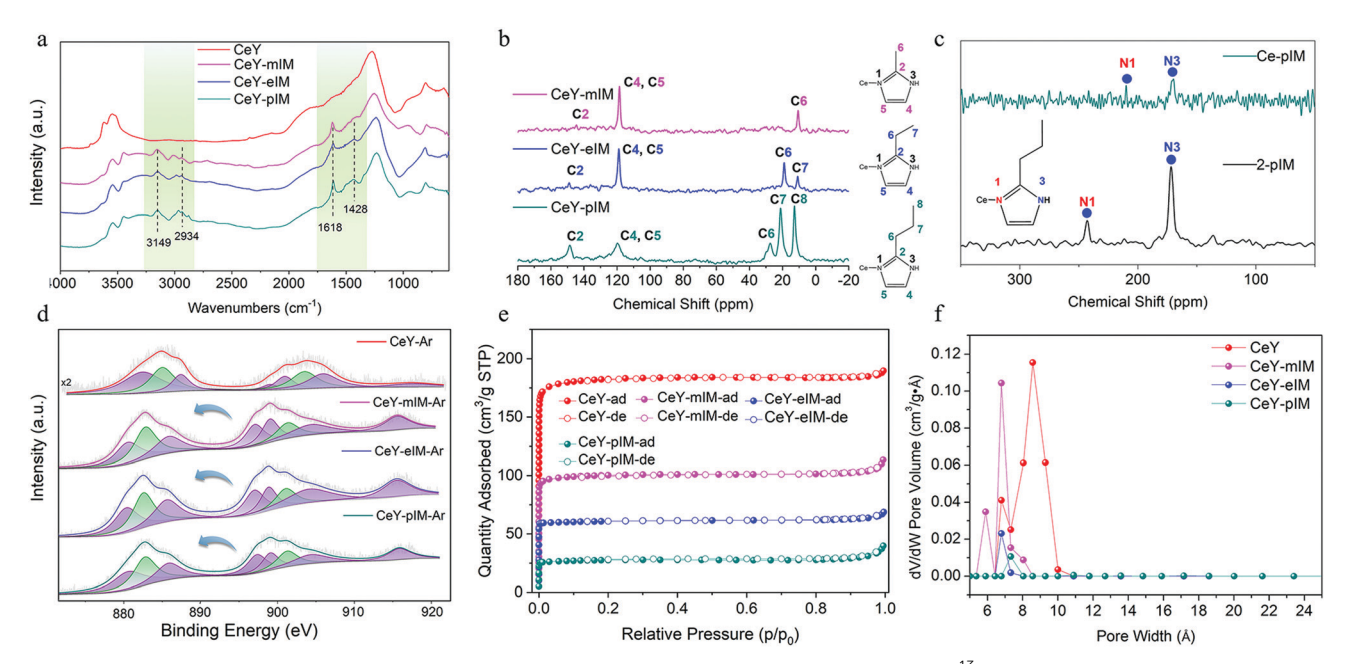


Fig. 1 (a) DRIFTS spectra of all the samples in a  $N_2$  environment at room temperature after dehydration. (b)  $^{13}$ C CP/MAS NMR spectra and assignment of the C environment of CeY-mIM, CeY-eIM and CeY-pIM. (c)  $^{15}$ N CP/MAS NMR spectra of pure pIM $^{19}$  and CeY-pIM. (d) Ce 3d XPS spectra of all the samples under an Ar atmosphere. (e)  $N_2$  adsorption–desorption isotherms of all the samples at -196 °C (adsorption: filled circles, desorption: hollow circles). (f) Pore size distributions of all the samples calculated using DFT.

**Materials Horizons** 

increased significantly compared with that of CeY; this result was attributed to the introduction of imidazole (Table S1, ESI†). In the diffuse reflectance FTIR (DRIFTS) spectra of the decorated samples (Fig. 1a), it was found that the bands at  $3149 \text{ cm}^{-1}$ ,  $2934 \text{ cm}^{-1}$  and  $1428 \text{ cm}^{-1}$  could be attributed to the C-H vibration of imidazole, and that the band at 1618 cm<sup>-1</sup> could be assigned to the vibration of the imidazole ring, which did not appear in the spectrum of CeY.<sup>23</sup> In addition, the <sup>13</sup>C CP/MAS NMR results (Fig. 1b) of the modified samples also characteristic resonances of imidazole molecules.20,21 A lower chemical shift was observed for N1 (210 ppm) than that for pure imidazole<sup>20</sup> in the <sup>15</sup>N CP/MAS NMR spectra (Fig. 1c); this difference in shifts is caused by the unique interaction between the Ce site and imidazole. The Ce 3d XPS spectra (Fig. 1d) of all the samples exhibited characteristic Ce  $3d_{3/2}$  and  $3d_{5/2}$  peaks that were consistent with those reported in the literature, 24 and the binding energy for the Ce 3d of the imidazole-modified samples shifted towards lower values compared with those of CeY. The 15N CP/MAS NMR and Ce 3d XPS results all indicated that the Ce-IM fragments in the decorated samples were formed by a bonding interaction. 20,21,25,26 It is worth noting that the Ce 3d XPS spectra showed that the valence state of some Ce ions changed from trivalent to tetravalent after modification. In the TGA curves of these samples (Fig. S4, ESI†), the imidazole-modified samples all exhibited two stages of weight loss, which represented the removal of water and the decomposition of imidazole, and a high decomposition temperature (500 °C). As for pure imidazole chemicals, they only experienced significant weight loss in the 200-220 °C range, which also indicated the presence of strong binding between the imidazole and Ce ions. The N<sub>2</sub> adsorption-desorption isotherms of all the samples at -196 °C were typical type-I sorption isotherms (Fig. 1e), which indicates that the CeY and decorated samples all had microporous characteristics. The Brunauer-Emmett-Teller (BET) micropore surface areas (Smicro) and the t-plot micropore volume  $(V_m)$  of all the samples were calculated and are compared in Table 1. CeY had the largest  $S_{\rm micro}$ and  $V_{\rm m}$ , and the  $S_{\rm micro}$  and  $V_{\rm m}$  of the decorated samples decreased as the molecular size of the introduced imidazole increased. The order of  $S_{
m micro}$  and  $V_{
m m}$  was CeY > CeY-mIM > CeY-eIM >CeY-pIM, and the pore size distributions calculated using density functional theory (DFT) showed that the modification with

The single-component  $O_2$  and  $N_2$  adsorption isotherms of CeY, CeY-mIM, CeY-eIM and CeY-pIM at 25  $^\circ$ C are shown in

imidazole significantly reduced the pore size of CeY (Fig. 1f).

The above results all indicate the successful decoration with

imidazole ligands.

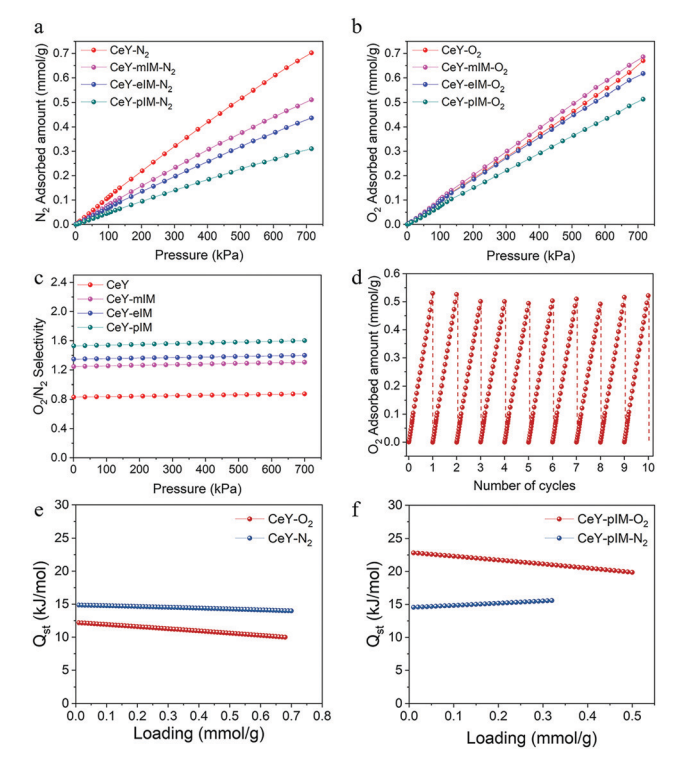


Fig. 2 (a)  $N_2$  and (b)  $O_2$  adsorption isotherms of the samples at 25 °C. (c) IAST-predicted selectivities for  $O_2/N_2$  mixtures (21:79) on the samples at 25 °C. (d) Cyclic regeneration experiments for  $O_2$  adsorption on CeY-pIM at 25 °C and pressures up to 715 kPa. (e) Isosteric heats of  $O_2$  and  $N_2$  adsorption on CeY-pIM.

Fig. 2, and the O<sub>2</sub> and N<sub>2</sub> uptake values on them at 715 kPa are listed in Table 1. For CeY, the N<sub>2</sub> uptake was slightly higher than that of O<sub>2</sub>, which indicates that it was still a N<sub>2</sub>-selective adsorbent. However, after modification with imidazole, the changes in the O2 and N2 uptake on these decorated samples were very interesting. The N2 uptake of CeY-mIM decreased compared with that of CeY, but its O2 uptake was higher than that of CeY. As a result, the O2 uptake on CeY-mIM was obviously higher than its N2 uptake. Considering the weakening of the electric field of the zeolite framework and the reduction in  $S_{\text{micro}}$  and  $V_{\text{m}}$  after decoration, this increase in  $O_2$  uptake in the decorated samples is abnormal, which suggests that there is a unique interaction between the imidazole-modified sample and O2 but not with N2. When CeY was modified with eIM and pIM, which have larger molecular sizes, the  $S_{\text{micro}}$  and  $V_{\text{m}}$  of these modified samples further reduced, and resulted in a decrease in O<sub>2</sub> and N<sub>2</sub> uptake on the obtained CeY-eIM and CeY-pIM samples compared to those on CeY-mIM. In Table 1, it can be

 Table 1
 Microporous and adsorption properties of all the samples

Sample	$S_{ m micro} \left( { m m}^2 \ { m g}^{-1}  ight)$	$V_{\rm m}$ (cm <sup>3</sup> g <sup>-1</sup> )	$ m N_2$ uptake at 715 kPa, 25 °C (mmol $g^{-1}$ )	${ m O_2}$ uptake at 715 kPa, 25 $^{\circ}{ m C}$ (mmol g $^{-1}$ )	IAST $O_2/N_2$ selectivity at 700 kPa, 25 $^{\circ}C$
CeY	537	0.26	0.702	0.670	0.9
CeY-mIM	295	0.14	0.512	0.686	1.3
CeY-eIM	181	0.09	0.437	0.618	1.4
CeY-pIM	76	0.04	0.311	0.514	1.6

Communication Materials Horizons

clearly seen that the reduction of O2 uptake was much lower than that of N<sub>2</sub> uptake, which ultimately resulted in an increase in O<sub>2</sub> selectivity towards N2. The above results all showed that there were special sites that could selectively bind to O2 in the modified samples. The ideal adsorbed solution theory (IAST)<sup>27</sup> was used to calculate the O<sub>2</sub>/N<sub>2</sub> selectivity of all the samples at 25 °C. The results (Fig. 2c and Table 1) showed that the O<sub>2</sub>/N<sub>2</sub> selectivity of CeY before modification was approximately 0.9, while the O<sub>2</sub>/N<sub>2</sub> selectivity of all three samples modified with imidazole was greater than 1 in the test pressure ranges; that is, the imidazole decoration changed CeY from the selective adsorption of N2 to the selective adsorption of O2. The O2/N2 selectivity order was CeY-mIM < CeY-eIM < CeY-pIM. The introduction of imidazole molecules can weaken the electric field of zeolite frameworks. Among the three imidazole molecules, pIM with the largest molecular size had the strongest negative effect on N2 adsorption, and thus CeY-pIM had the highest O<sub>2</sub>/N<sub>2</sub> selectivity (1.6 at 700 kPa). The cycling performance of the CeY-pIM sample is shown in Fig. 2d. The desorption step in each cycle was achieved by outgassing at 200 °C under high vacuum conditions for 2 h. The results showed that after 10 adsorption-desorption cycles, the O2 adsorption capacity of the CeY-pIM sample was well maintained, which indicates that this adsorbent has great application potential in O2/N2 separation. It is worth noting that after desorption with relatively low temperatures (100 °C and 25 °C), CeY-pIM displayed a loss (about 15%) in capacity, but this loss can be eliminated through increasing the desorption temperature to 200 °C (Fig. S5, ESI†). In addition, the isosteric heat of adsorption (Qst) of CeY and CeY-pIM was calculated using the Clausius-Clapeyron equation<sup>28</sup> (see the ESI†). As shown in Fig. 2e, the  $Q_{\rm st}$  of  $O_2$  for CeY was lower than that of  $N_2$ , which indicates that the interaction between CeY and N2 is stronger than that for O2. However, CeY-pIM has a higher O2 adsorption heat than N2 adsorption heat (Fig. 2f), which means that the decorated sample thermodynamically prefers to adsorb O2 over N2. The Qst of O2 for CeY-pIM is obviously higher than that of CeY, and suggests that the decoration enhances the interaction of the adsorbent with O2. Furthermore, Fig. 2f shows that the Q<sub>st</sub> of O<sub>2</sub> adsorption is relatively low compared with some MOFs that bind O2 through chemical adsorption (>40 kJ mol<sup>-1</sup>), <sup>12,13</sup> indicating that O<sub>2</sub> adsorption is still in the physical adsorption range, which is also the reason why CeY-pIM has good cycling performance.

In addition, breakthrough experiments with binary mixtures of  $O_2/N_2$  (21:79, v/v) were carried out to further verify the performance of the imidazole-modified adsorbent for  $O_2/N_2$  separation. The breakthrough curves of CeY and CeY-pIM, which had the highest  $O_2/N_2$  selectivity, are shown in Fig. 3. Unmodified CeY had almost no  $O_2/N_2$  separation performance, and  $O_2$  eluted from the packed bed faster than  $N_2$ . For the CeY-pIM sample,  $N_2$  achieved a fast breakthrough at approximately 110 s, while  $O_2$  was retained in the packed bed until 196 s. Regeneration and circulation of CeY-pIM can be achieved with heat treatment and He flow. After three cycles, the  $O_2/N_2$  selectivity of CeY-pIM was maintained (Fig. S9, ESI†). This result indicated that the interaction between the imidazole-

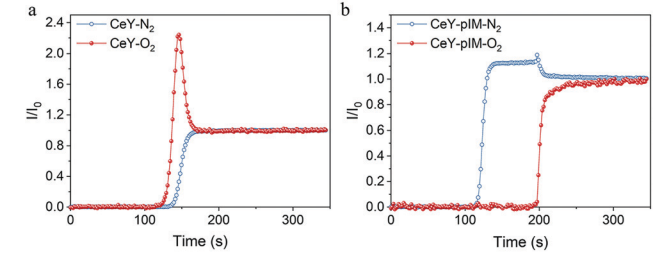


Fig. 3 Breakthrough curves of  $O_2/N_2$  (21:79, v/v) mixtures on (a) CeY, (b) CeY-pIM at 25  $^{\circ}$ C and 100 kPa.

modified sample and  $O_2$  at room temperature is reversible, and suggests that the imidazole-modified sample has good application prospects.

To further study and confirm the interaction mechanism between the imidazole-modified samples and O2, in situ XPS characterizations were carried out. CeY and CeY-pIM were activated by heating in a vacuum prior to testing their N2 or O<sub>2</sub> adsorption at 25 °C and 0.1 kPa, and the results are shown in Fig. 4. The Ce 3d binding energy of CeY does not change after adsorbing O2 and N2 compared with that in an inert Ar atmosphere, which indicates that the Ce site of CeY does not exhibit obvious electron transfer to the O2 and N2 molecules. The Ce 3d binding energy of CeY-pIM after adsorbing N2 also did not change, but its Ce 3d binding energy after adsorbing O2 shifted towards higher values than those under an Ar and N2 atmosphere. This important phenomenon indicates that the Ce sites of CeY-pIM have unique electron transfer interactions with  $O_2$ , and that more electrons are transferred to  $O_2$ . In addition, a molecular DFT simulation was carried out to simulate the interaction between O2/N2 and the Ce sites of the samples, and the Ce/Si-O-Al (Fig. 5a and b) and Ce-pIM/Si-O-Al (Fig. 5c and d) clusters were used to simplify the Ce sites of CeY and CeY-pIM, respectively (see the ESI†). The electron density difference of the O<sub>2</sub> and N<sub>2</sub> adsorption in the simplified clusters was then analyzed. As shown in Fig. 5, there is more electron transfer from the Ce-pIM/Si-O-Al cluster to O2 than from the Ce/Si-O-Al cluster, and both of them exhibited almost no electron transfer to N2, which is consistent with the in situ XPS results. The Ce-N distances of the Ce-pIM/Si-O-Al cluster under different conditions calculated in the simulations are shown in Fig. S14 (ESI†). The results also indicate that the Ce-pIM/Si-O-Al cluster has electron transfer interactions with

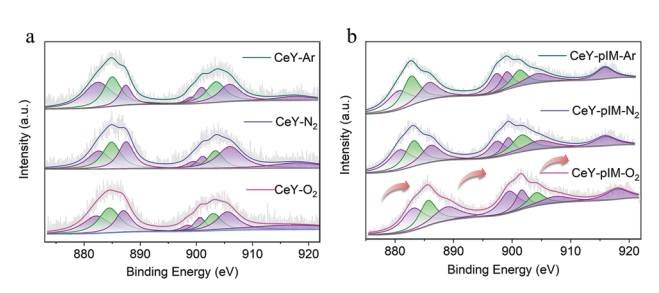


Fig. 4 In situ Ce 3d XPS spectra of (a) CeY and (b) CeY-pIM under an atmosphere of different gases at 25  $^{\circ}$ C and 0.1 kPa.

**Materials Horizons** Communication

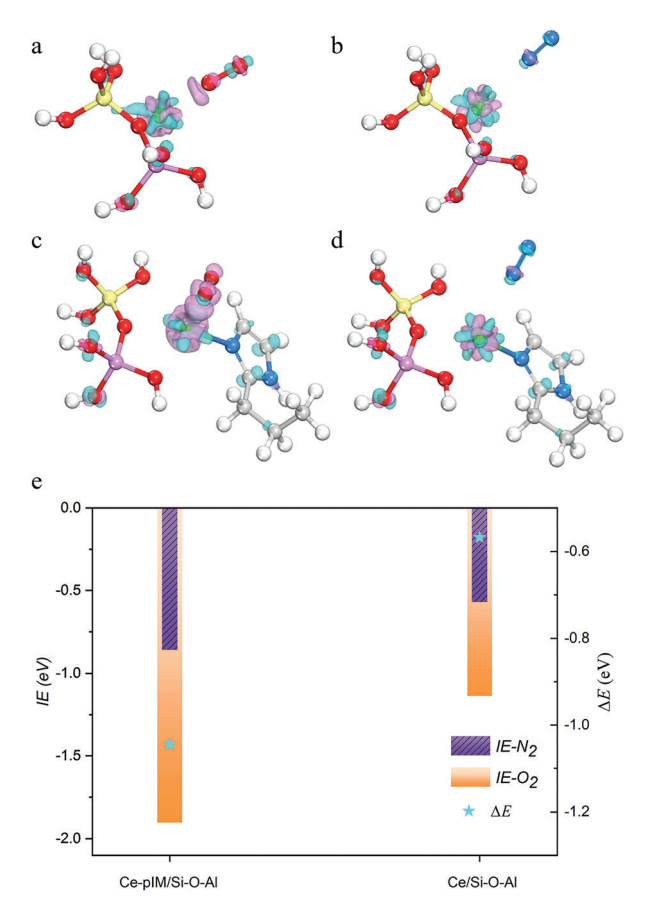


Fig. 5 Electron density difference of O<sub>2</sub> and N<sub>2</sub> adsorption in the Ce/Si-O-Al cluster of CeY (a and b) and the Ce-pIM/Si-O-Al cluster of CeY-pIM (c and d). The light purple and cyan surfaces represent a gain or loss of electron density, respectively (isosurface value = 0.09 e<sup>-</sup> bohr<sup>-3</sup>, Ce: green, O: red, N: light blue, Si: yellow, Al: violet, C: brown, H: white). (e) The interaction energies (IE) between the simplified clusters and  $O_2$  or  $N_2$ , and the difference between IE-O<sub>2</sub> and IE-N<sub>2</sub> ( $\Delta E$ ).

O<sub>2</sub> (see the ESI†). The interaction energies (IE) between the above two clusters and O2 (IE-O2) or N2 (IE-N2) molecules were also calculated. As shown in Fig. 5e, we found that the IE-O<sub>2</sub> (-1.9 eV) of Ce-pIM/Si-O-Al is lower than the IE-O<sub>2</sub> (-1.1 eV) of Ce/Si-O-Al, which indicates that the binding ability of O<sub>2</sub> at CeY-pIM is stronger than that of CeY. In addition,  $\Delta E$  was defined as the difference between IE-O2 and IE-N2, and we found that the  $\Delta E$  above Ce-pIM/Si-O-Al was larger than that above Ce/Si-O-Al, which indicates that compared with CeY, the binding ability difference of O2 and N2 on the Ce sites of the decorated samples is more significant. Based on the above results, we can conclude that the Ce sites within CeY are activated after decoration, which allows them to preferentially transfer electrons to O2 over N2, thereby enhancing the adsorption of  $O_2$ . For the above reason, even if the  $S_{\text{micro}}$  and  $V_{\rm m}$  of these samples were reduced and the framework electric field was weakened after imidazole modification, their O2 uptake was still higher than that of N2. Compared with MOF adsorbents (Table S3, ESI†), the decorated samples in this work have a relatively low O<sub>2</sub> adsorption capacity and selectivity. However, they have good stability, regenerability and especially

an outstanding dynamic separation ability at ambient temperature, which will make them have potential in practical applications.

#### Conclusions

In conclusion, we successfully transformed CeY that selectively adsorbs N2 into an O2-selective adsorbent by directly decorating the Ce sites with imidazole molecules, which gave rise to a novel O2 adsorbent and preparation method. The results showed that binding of the decorated samples to O2 was stronger than the binding to N2. The O2/N2 IAST selectivity of all the decorated samples was greater than 1, and the selectivity of the CeY-pIM sample was 1.6 (25 °C, 700 kPa). Breakthrough experiments clearly showed that O<sub>2</sub> eluted from the packed bed much later than N2 and that the adsorbents could be fully regenerated using heat treatment, which indicated the application potential of the adsorbent. In situ XPS experiments revealed that substantial electron transfer occurs between the Ce sites of the decorated samples and O2, which was further confirmed by molecular simulations. The strategy of decorating the metal sites of zeolites with organic molecules is expected to lead to the development of other efficient adsorbents.

#### Author contributions

Y. Xu and H. Liu planed the experiments. H. Liu carried out the relevant experiments and theoretical calculations. D. Yuan provided guidance for the breakthrough experiments. L. Yang and J. Xing revised the draft manuscript. S. Zeng and S. Xu provided help with the <sup>13</sup>C and <sup>15</sup>N CP/MAS NMR experiments. Y. Xu and Z. Liu initialized and supervised the project. All authors discussed the results and commented on the manuscript.

#### Conflicts of interest

There are no conflicts to declare.

## **Acknowledgements**

This work was supported by the National Natural Science Foundation of China (Grant No. 21802136) and the Talent Program for Revitalization of Liaoning Province (XLYC1905017).

#### References

- 1 R. T. Yang, Adsorbents fundamentals and applications, Wiley, New York, 2003.
- 2 W. F. Castle, Int. J. Refrig., 2002, 25, 158-172.
- 3 N. D. Hutson, S. U. Rege and R. T. Yang, AIChE J., 1999, 45, 724-734.
- 4 T. R. Gaffney, Curr. Opin. Solid State Mater. Sci., 1996, 1, 69-75.
- 5 Y. Tang, X. Wang, Y. Wen, X. Zhou and Z. Li, Ind. Eng. Chem. Res., 2020, 59, 6219-6225.
- 6 Y. Wang and R. T. Yang, ACS Sustainable Chem. Eng., 2019, 7, 3301-3308.

Communication **Materials Horizons** 

- 7 A. Jayaraman, R. T. Yang, S. H. Cho, T. S. G. Bhat and V. N. Choudary, Adsorption, 2002, 8, 271-278.
- 8 H. Juntgen, K. Knoblauch and K. Harder, Fuel, 1981, 60, 817-822.
- 9 S. P. Nandi and P. L. Walker, Sep. Sci., 1976, 11, 441-453.
- 10 D. Chen and A. E. Martell, Inorg. Chem., 1987, 26, 1026-1030.
- 11 D. Chen, A. E. Martell and Y. Z. Sun, Inorg. Chem., 1989, 28, 2647-2652.
- 12 E. D. Bloch, L. J. Murray, W. L. Queen, S. Chavan, S. N. Maximoff, J. P. Bigi, R. Krishna, V. K. Peterson, F. Grandjean, G. J. Long, B. Smit, S. Bordiga, C. M. Brown and J. R. Long, J. Am. Chem. Soc., 2011, 133, 14814-14822.
- 13 D. J. Xiao, M. I. Gonzalez, L. E. Darago, K. D. Vogiatzis, E. Haldoupis, L. Gagliardi and J. R. Long, J. Am. Chem. Soc., 2016, 138, 7161-7170.
- 14 E. D. Bloch, W. L. Queen, M. R. Hudson, J. A. Mason, D. J. Xiao, L. J. Murray, R. Flacau, C. M. Brown and J. R. Long, Angew. Chem., Int. Ed., 2016, 55, 8605-8609.
- 15 L. J. Murray, M. Dinca, J. Yano, S. Chavan, S. Bordiga, C. M. Brown and J. R. Long, J. Am. Chem. Soc., 2010, 132, 7856-7857.
- 16 Y. Shang, J. Wu, J. Zhu, Y. Wang and C. Meng, J. Alloys Compd., 2009, 478, 5-7.
- 17 G. Sethia, R. S. Pillai, G. P. Dangi, R. S. Somani, H. C. Bajaj and R. V. Jasra, Ind. Eng. Chem. Res., 2010, 49, 2353-2362.

- 18 S. A. Peter, J. Sebastian and R. V. Jasra, Ind. Eng. Chem. Res., 2005, 44, 6856-6864,
- 19 H. Liu, D. Yuan, G. Liu, J. Xing, Z. Liu and Y. Xu, Chem. Commun., 2020, 56, 11130-11133.
- 20 Y. Q. Wu, D. H. Yuan, D. W. He, J. C. Xing, S. Zeng, S. T. Xu, Y. P. Xu and Z. M. Liu, Angew. Chem., Int. Ed., 2019, 58, 10241-10244.
- 21 Y. Wu, S. Zeng, D. Yuan, J. Xing, H. Liu, S. Xu, Y. Wei, Y. Xu and Z. Liu, Angew. Chem., Int. Ed., 2020, 59, 6765-6768.
- 22 J. Sebastian and R. V. Jasra, Ind. Eng. Chem. Res., 2005, 44, 8014-8024.
- 23 A. M. Ebrahim, A. M. Plonka, N. Rui, S. Hwang, W. O. Gordon, A. Balboa, S. D. Senanayake and A. I. Frenkel, ACS Appl. Mater. Interfaces, 2020, 12, 58326-58338.
- 24 J. J. He, Y. H. Xu, W. Wang, B. Hu, Z. J. Wang, X. Yang, Y. Wang and L. W. Yang, Chem. Eng. J., 2020, 379.
- 25 L. T. A. Sofia, A. Krishnan, M. Sankar, N. K. K. Raj, P. Manikandan, P. R. Rajamohanan and T. G. Ajithkumar, J. Phys. Chem. C, 2009, 113, 21114-21122.
- 26 E. F. Baxter, T. D. Bennett, C. Mellot-Draznieks, C. Gervais, F. Blanc and A. K. Cheetham, Phys. Chem. Chem. Phys., 2015, 17, 25191-25196.
- 27 A. L. Myers and J. M. Prausnitz, AIChE J., 1965, 11, 121-127.
- 28 Y. Zhang, H. Xiao, X. Zhou, X. Wang and Z. Li, Ind. Eng. Chem. Res., 2017, 56, 8689-8696.